

# Finite-temperature superconducting correlations of the Hubbard model

Ehsan Khatami,<sup>1,2</sup> Richard T. Scalettar,<sup>1</sup> and Rajiv R. P. Singh<sup>1</sup>

<sup>1</sup>*Department of Physics, University of California, Davis, CA 95616, USA*

<sup>2</sup>*Department of Physics and Astronomy, San Jose State University, San Jose, CA 95192, USA*

We utilize numerical linked-cluster expansions (NLCEs) and the determinantal quantum Monte Carlo algorithm to study pairing correlations in the square lattice Hubbard model. To benchmark the NLCE, we first locate the finite-temperature phase transition of the attractive model to a superconducting state away from half filling. We then explore the superconducting properties of the repulsive model for the  $d$ -wave and extended  $s$ -wave pairing symmetries. The pairing structure factor shows a strong tendency to  $d$ -wave pairing and peaks at an interaction strength comparable to the bandwidth. The extended  $s$ -wave structure factor and correlation length are larger at higher temperatures but clearly saturate as temperature is lowered, whereas the  $d$ -wave counterparts, which start off lower at high temperatures, continue to rise near half filling. This rise is even more dramatic in the  $d$ -wave susceptibility. The convergence of NLCEs breaks down as the susceptibilities and correlation lengths become large, so we are unable to determine the onset of long-range order. However, our results extend the conclusion, previously restricted to only magnetic and charge correlations, that NLCEs offer unique window into pairing in the Hubbard model at strong coupling.

PACS numbers: 71.10.Fd, 74.72.-h, 67.85.-d, 05.10.-a

## I. INTRODUCTION

Despite several decades of intensive theoretical research, the question of whether a non-local attraction can dominate in a fermionic Hubbard model with local repulsive interaction has remained largely unanswered for parameters relevant to cuprate high-temperature superconductors.<sup>1–6</sup> Controlled theoretical approaches confirm this possibility, however, only when the strength of the local repulsion is much smaller than the hopping amplitude of fermions on a square lattice.<sup>7</sup>

Numerical methods provide important data for strongly-correlated quantum Hamiltonians, and, in particular, for phenomena like superconductivity, magnetism, and Mott metal-insulator transitions. Although many developments have made these approaches increasingly powerful over the last decade, significant limitations remain, especially for fermions. The density matrix renormalization group,<sup>8,9</sup> and related techniques, function best in one dimension. Diagrammatic quantum Monte Carlo techniques<sup>10,11</sup> are restricted to weak-coupling regimes. Determinant quantum Monte Carlo (DQMC),<sup>12,13</sup> and cluster extensions of the dynamic mean-field theory<sup>14,15</sup> are limited to real space or momentum space clusters of tens to hundred of sites. Moreover, the “sign problem”<sup>16,17</sup> remains an unsolved problem which limits accessible temperatures unless special symmetries prevail.

These limitations emphasize the need for continued algorithm development. Recently developed numerical linked-cluster expansions (NLCEs)<sup>18–21</sup> are especially promising as an approach to access strong coupling regimes, which are inaccessible to QMC methods, as a consequence both of the sign problem and of large and even diverging statistical fluctuations. For instance, analysis of magnetic correlations and Mott phases in trapped atoms on optical lattices,<sup>22,23</sup> where strong

coupling is present at the cloud edge, would not have been possible without NLCEs.

A natural next step is the application of NLCEs to superconductivity. In this Rapid Communication, we show this method can be developed and successfully used to study the pairing correlations in the square lattice Hubbard model,

$$H = -t \sum_{\langle ij \rangle \sigma} c_{i\sigma}^\dagger c_{j\sigma} + U \sum_i n_{i\uparrow} n_{i\downarrow} - \mu \sum_{i\sigma} n_{i\sigma}, \quad (1)$$

where  $c_{i\sigma}$  ( $c_{i\sigma}^\dagger$ ) annihilates (creates) a fermion with spin  $\sigma$  on site  $i$ ,  $n_{i\sigma} = c_{i\sigma}^\dagger c_{i\sigma}$  is the number operator,  $U$  is the onsite Coulomb interaction, and  $t$  is the near neighbor hopping integral. We set  $k_B = 1$ , and  $t = 1$  as the unit of energy throughout the paper.

We complement our NLCE results with those obtained from (numerically unbiased) DQMC simulations on a large lattice. We find excellent agreement between the two in parameter regions accessible to both, and show that the lowest temperatures achievable in the NLCE are similar to, or often lower than, those of the DQMC. For the attractive model ( $U < 0$ ), or in the weak-coupling regime of the repulsive model, where the sign problem is either absent or less severe, DQMC can generally access lower temperatures than the NLCE. On the other hand, the series converges to lower temperatures in the strong-coupling regime, where DQMC runs into sampling difficulties and faces an unforgiving sign problem.

We find that, for an interaction strength  $U$  equal to the bandwidth, the  $s$ -wave pairing structure factor of the attractive model away from half filling shows divergent behavior at low temperatures, and points to a finite transition temperature that is consistent with findings of previous large-scale DQMC studies.<sup>24–28</sup> For the repulsive model, we consider several values of  $U$  and doping and study pairing in the nonlocal channels

of extended  $s$ -wave ( $s^*$ -wave) and  $d$ -wave. While the structure factor for the former symmetry tends to saturate at increasingly high temperatures as the doping is increased, for the latter symmetry, no such tendency is observed. We examine results at 10% doping more closely and find that the low-temperature structure factor is maximum around  $U = 8$ . On the other hand, the pair-field susceptibility, while larger for smaller values of  $U$  in the intermediate temperature region, shows a sharp upturn at the lowest accessible temperatures for the largest interactions considered.

## II. NUMERICAL METHODS

In NLCEs, an extensive property of the lattice model, when normalized to the number of sites, is expressed in the thermodynamic limit in terms of contributions from finite clusters of various sizes and topologies that can be embedded in the lattice. Thus, NLCEs use the same basis as the high-temperature expansions (HTEs). However, the calculation of the extensive quantities at the level of individual clusters is left to an exact numerical method, such as exact diagonalization, as opposed to a perturbative expansion in terms of inverse temperature in the HTEs. A typical expansion involves clusters up to a certain size that are chosen according to a self-consistent criterion (see below). Despite the lack of an explicit small parameter, having a finite number of clusters in the series inevitably leads to the loss of convergence below a certain temperature, where the correlations in the system extend beyond a length of the order of the largest sizes considered. However, the exact treatment of clusters leads to convergence temperatures that are lower than those of HTE with a comparable number of orders.

Similar to the analytic Padé approximations used extensively in HTEs, here we take advantage of two *numerical* resummation techniques to improve the convergence of our series at low temperatures. We use the Euler algorithm<sup>29</sup> to resum the last 4-6 terms of the series or the Wynn algorithm<sup>30</sup> with 3 and 4 cycles of improvement (details of these techniques can be found in Ref. 19). We then take the average of four values, the last two orders after the Euler and the last two orders after the Wynn transformations, as our best estimate. To quantify our confidence in the accuracy of the resummed results, we define a “confidence region” around this average where all the values that contribute to the average fall. Thus, the errorbars in our figures simply mark the boundaries of this region and should not be confused with statistical errorbars.

We study the superconducting properties of the model at several values of the interaction strength and on a fine grid of temperature and chemical potential. The latter allows us to study the calculated quantities at constant electronic densities after numerical conversion. As with previous studies of Hubbard models using the NLCE,<sup>31–33</sup> we employ the site expansion in which the

order to which each cluster belongs is determined by the number of sites it has. In order  $l$ , we consider all the open boundary clusters of various shapes and topologies on the square lattice that have  $l$  sites, and use exact diagonalization to solve for their properties. For the pairing correlations, the Hamiltonian matrices are block-diagonalized in each particle number sector. So, we are able to carry out the expansion to the ninth order. For the pairing susceptibility, on the other hand, we can only carry out the expansion to the seventh order since not only particle number is not conserved during the time-dependent measurements (see Eq. 6), but also the majority of the computational time is spent on obtaining the off-diagonal expectation values, which, like the diagonalization, scales like  $O(N^3)$ .<sup>34</sup>

DQMC simulations are performed on a  $10 \times 10$  lattice, which is large enough to have only small finite size effects at the temperatures studied here. Results represent averages of at least 8 independent runs with 10,000 sweeps each. To fix the density,  $n$ , away from half filling at each temperature and  $U$  value, the chemical potential needs to be tuned starting from an estimate provided by the NLCE. Therefore, we repeat the calculations for several values of  $\mu$  to achieve an accuracy of about 0.01% for the density. For the structure factor, we extrapolate our results to the continuous imaginary time limit using the outcome of two separate simulations with a discretization of the inverse temperature  $\beta = L\Delta\tau$  corresponding to  $\Delta\tau = 1/16$  and  $1/12$ . In the case of the susceptibility, we choose an even smaller  $\Delta\tau = 1/50$ , in order to perform the imaginary time integration accurately. This value leads to Trotter errors that are negligible in comparison to the statistical ones.

One of the quantities we calculate is the equal-time pairing structure factor,

$$S^\alpha(\mathbf{q}) = \sum_{\mathbf{r}} e^{i\mathbf{q}\cdot\mathbf{r}} P^\alpha(\mathbf{r}), \quad (2)$$

where

$$P^\alpha(\mathbf{r}_{ij}) = \langle \Delta_i^{\alpha\dagger}(0) \Delta_j^\alpha(0) + \Delta_i^\alpha(0) \Delta_j^{\alpha\dagger}(0) \rangle \quad (3)$$

is the equal-time pair-pair correlation function. Here, the pairing operator for the symmetry  $\alpha$  is defined as

$$\Delta_i^\alpha(\tau) = \frac{1}{2} \sum_j f_{ij}^\alpha e^{\tau H} (c_{i\uparrow} c_{j\downarrow} - c_{i\downarrow} c_{j\uparrow}) e^{-\tau H}. \quad (4)$$

We consider three pairing symmetries in this study; (local)  $s$ -wave,  $d$ -wave, and  $s^*$ -wave. For the  $s$ -wave symmetry,  $f_{ij}^s = \delta_{ij}$ . In the case of  $s^*$ -wave,  $f_{ij}^{s^*}$  is +1 if  $i$  and  $j$  are nearest neighbors and  $j > i$  (to avoid double counting) and zero otherwise.  $f_{ij}^d$  for the  $d$ -wave symmetry is the same as  $f_{ij}^{s^*}$  except it takes the value  $-1$  if the bond connecting  $i$  and  $j$  is along the  $y$  axis. Here, we consider only the uniform pairing structure factor,  $S^\alpha(\mathbf{q} = 0)$ . The correlated structure factors,  $S_{\text{corr}}^\alpha$ , is obtained by first subtracting off the uncorrelated parts of the expressions in Eq. 3.<sup>35</sup>

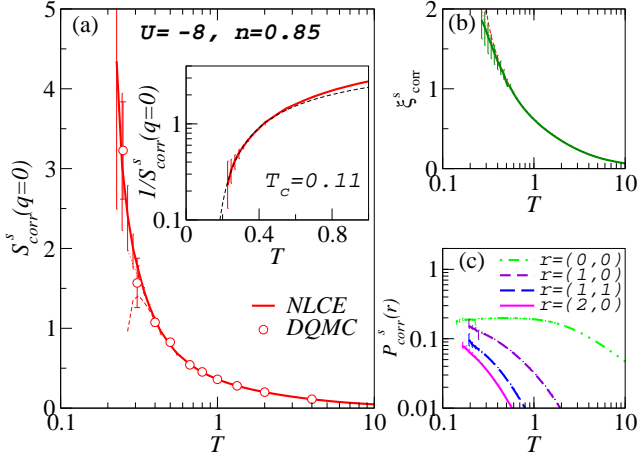


FIG. 1. (a) Temperature dependence of the  $s$ -wave pairing structure factor at  $n = 0.85$  for the attractive model with  $U = -8$ . The line is from NLCE and symbols are from DQMC. The inset shows the inverse of the same function vs  $T$  and a low-temperature fit to  $A \exp(B/\sqrt{T-T_c})$  with  $T_c = 0.11$ . (b)-(c) The corresponding correlation length and short-range correlation functions vs  $T$ . In the main panel of (a) and in (b), bare NLCE results before resummations for the last two orders, 8<sup>th</sup> and 9<sup>th</sup>, are shown as thin dotted and dashed lines, respectively.

Having the uniform structure factor ( $S^\alpha$  or  $S_{\text{corr}}^\alpha$ ), the corresponding correlation length,  $\xi$ , can also be calculated using, e.g.,

$$(\xi_{\text{corr}}^\alpha)^2 = \frac{1}{2d S_{\text{corr}}^\alpha(\mathbf{q}=0)} \sum_i |\mathbf{r}_i|^2 P_{\text{corr}}^\alpha(\mathbf{r}_{0i}), \quad (5)$$

where  $d = 2$  is the dimension.

The other quantity of interest for superconductivity is the uniform pairing susceptibility, which is defined as

$$\chi^\alpha = \frac{1}{N} \int_0^\beta d\tau \langle \mathcal{O}^\alpha(\tau) \mathcal{O}^{\alpha\dagger}(0) \rangle, \quad (6)$$

where  $\mathcal{O}^\alpha(\tau) = \sum_i \Delta_i^\alpha(\tau)$ .

### III. RESULTS

We start with the attractive Hubbard model, for which we know there exists a finite-temperature Kosterlitz-Thouless (KT) phase transition to an  $s$ -wave superconducting state away from half filling.<sup>24–28</sup> In Fig. 1(a), we show the correlated part of the  $s$ -wave pairing structure factor from the NLCE for  $U = -8$  and at  $n = 0.85$ , where the superconducting transition temperature is expected to be maximal.<sup>26</sup> Results are in excellent agreement with the corresponding DQMC results, plotted as empty circles in that figure. As can be inferred from previous DQMC simulations with a smaller  $U$ ,<sup>26</sup> finite-size effects in DQMC will not play a role here at temperatures as low as  $T = 0.25$ . Whereas the raw

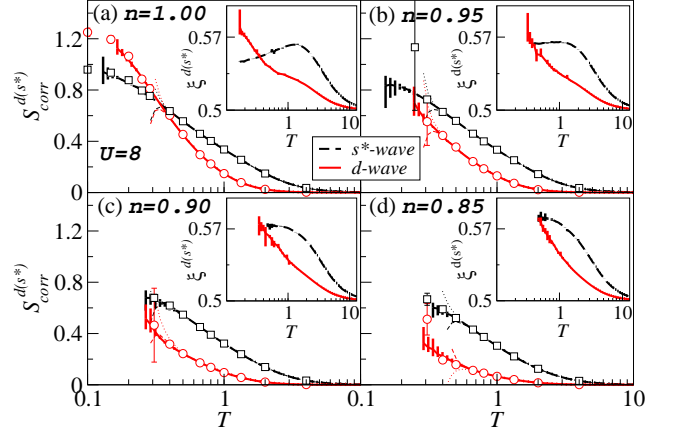


FIG. 2. The uniform  $d$ -wave and extended  $s$ -wave pairing structure factors for the repulsive model with  $U = 8$  at densities 1.00, 0.95, 0.90, and 0.85 vs temperature. Lines are from the NLCE and symbols are from the DQMC. Bare NLCE results before resummations for the 8<sup>th</sup> and 9<sup>th</sup> orders, are shown as thin dotted and dashed lines, respectively. The insets show the correlation lengths from the NLCE vs temperature for each case.

NLCE results (before resummations) converge only to  $T \sim 0.4$ , the averaged value after resummations suggest a divergent behavior for  $S_{\text{corr}}^s$  at lower temperatures. They lead us to a regime where we can take advantage of extrapolations in temperature in order to obtain an estimate for the critical temperature. We find that a fit to the KT form [see the inset of Fig. 1(a)], leads to  $T_c \sim 0.11$ , which is in good agreement with results of past DQMC simulations.<sup>24</sup> The correlation length, which shows an exponential growth, is also plotted in Fig. 1(b). Its behavior is consistent with the trend seen in Fig 1(c) for the pairing correlations growing faster at longer length scales as the temperature is decreased.

We now turn our focus to the main subject of this study; pairing in the repulsive Hubbard model. We know that if a similar finite-temperature transition to a superconducting phase takes place in the latter model, the pairing symmetry has to be nonlocal because of the onsite Coulomb repulsion. Therefore, in this case, we only explore the  $d$ -wave and the  $s^*$ -wave symmetries. We also expect the corresponding temperature scales to be much smaller than those for the attractive model since we are looking for attraction in a repulsive model.

In Fig. 2, we show the correlated part of the uniform structure factor for the two pairing symmetries when  $U = 8$  and at various average densities. At half filling, the series converges to a low enough temperature to make clear that  $S_{\text{corr}}^\alpha$  eventually saturates as we decrease the temperature. In the absence of the ‘sign problem’ at this filling, DQMC can easily access lower temperatures. We see in Fig. 2(a) that, while agreeing excellently with NLCE at high temperatures, results from DQMC simulations confirm the saturation at lower  $T$ . As we move away from half filling into the hole-doped region

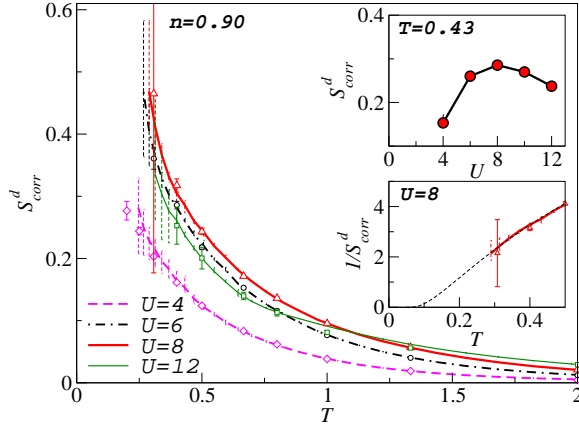


FIG. 3. Temperature dependence of the  $d$ -wave pairing structure factor at  $n = 0.90$  for  $U = 4, 6, 8$ , and  $12$ . Symbols are the DQMC results. Top inset shows the same structure factor vs  $U$  at a fixed temperature  $T = 0.43$ . The bottom inset shows the inverse of the structure factor vs  $T$ , along with a fit to the function  $A \exp(B/\sqrt{T - T_c})$  for  $T < 0.6$ , which results in  $T_c = 0.048$ .

( $n < 1.0$ ), an interesting trend is observed; the saturation of the  $s^*$ -wave structure factor is seen to take place at higher temperatures whereas the  $d$ -wave structure factor continues to grow at the lowest temperatures accessible to us, although its over all values decrease as we increase the doping. Hence, if there is an instability to pairing away from half filling in this model, it would be in the  $d$ -wave and not the  $s^*$ -wave channel. Interestingly, at small dopings near half filling, NLCE results are more reliable at generally lower temperatures than those of the DQMC because of the restrictions imposed by a severe sign problem in this region [see Fig. 2(b)]. Nevertheless, results from the two methods match within the errorbars at the available temperatures for all the dopings studied.

The favorability of  $d$ -wave over  $s^*$ -wave pairing is also evidenced by the behavior of the corresponding correlation lengths, shown in the insets of Fig. 2. For example, even though the low-temperature  $s^*$ -wave structure factor is larger than the  $d$ -wave one away from half filling, its correlation length clearly saturates while that of the  $d$ -wave keeps rising and becomes larger. The latter can explain the higher convergence temperature of  $S_{\text{corr}}^{s^*}$  in comparison to  $S_{\text{corr}}^d$  in Fig. 2(b).

Focusing on  $d$ -wave pairing at a moderately doped system with  $n = 0.9$ , we find that at temperatures below one, the structure factor is largest at  $U \sim 8$ , which is equal to the non-interacting bandwidth. This can be seen in Fig. 3, where we show  $S_{\text{corr}}^d$  vs temperature for  $U = 4, 6, 8$ , and  $12$ . For  $U = 4$ , the DQMC results are available at lower temperatures than the NLCE and show a relatively slow increase of this quantity as the temperature is decreased. In the top inset of Fig. 3, we see that the structure factor at  $T = 0.43$  quickly rises as  $U$  increases from 4, reaches a maximum at  $U = 8$ , and then slowly decreases. Beyond  $U = 12$ ,

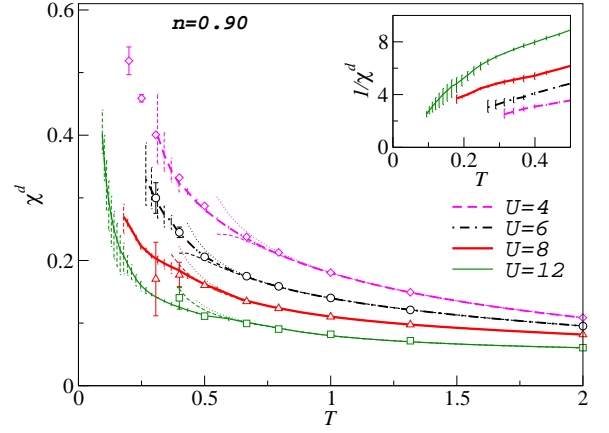


FIG. 4. The  $d$ -wave pairing susceptibility at  $n = 0.90$  vs temperature for  $U = 4, 6, 8$ , and  $12$ . Bare NLCE results before resummations for the last two orders, 6<sup>th</sup> and 7<sup>th</sup>, are shown as thin dotted and dashed lines, respectively. Symbols are the DQMC results. The inset shows the inverse of the susceptibility vs temperature for the same values of the interaction strength.

we expect this quantity to scale as  $1/U$  as, in the strong-coupling regime, the only relevant energy scale will be the exchange interaction of the corresponding low-energy  $t - J$  model,  $J = 4t^2/U$ . The bottom inset in Fig. 3 shows the inverse of the structure factor at  $U = 8$ . Unfortunately, we are not close enough to a transition temperature to be able to make any quantitative statement about its value. However, the best estimate from the DCA for a close value of the interaction ( $U = 7$ ), puts  $T_c$  around  $0.05$ ,<sup>28</sup> which is consistent with a KT fit to our results for  $T < 0.6$ .

Finally, we turn to the pair-field susceptibility. Figure 4 shows  $\chi^d$  vs temperature at  $n = 0.9$  for different interaction strengths. Our results for the susceptibilities match the DQMC ones very well for smaller  $U$  values and for larger  $U$  values when the temperature is not too low. This includes the susceptibility at  $U = 4$  and  $n = 0.875$ <sup>36</sup> (not shown). In all cases, there is a rapid increase in the susceptibility at low temperatures. However, more terms are needed for the susceptibility to capture the sharp rise at low temperatures, and to determine how  $T_c$  may depend on  $U$ . In future, it would be important to extend the results for the susceptibility to higher orders and also calculate pairing susceptibilities at non-zero momenta.

In summary, we have employed two unbiased methods, the NLCE and the DQMC to study finite-temperature superconducting properties of the square lattice Fermi-Hubbard model. To benchmark our NLCE approach, we first explore the  $s$ -wave pairing in the attractive model away from half filling. By fitting our low-temperature pairing structure factor to known forms, we obtain a  $T_c$  that is consistent with the best estimate from large-scale QMC simulations. We then investigate the nonlocal  $s^*$ -wave and  $d$ -wave pairing instabilities in the repulsive model at various dopings and for several interaction



strengths. We find that the  $d$ -wave symmetry has the tendency to be dominant at low temperatures and that its structure factor has a maximum at  $U \sim 8$ . We also calculate the pairing susceptibility, which shows a similar divergent behavior in the  $d$ -wave channel and a sharp upturn at low temperatures for large interactions.

An important potential application of the results described here is to ongoing emulation of model Hamiltonians which describe fermionic atoms in optical lattices. NLCEs allow the rapid evaluation of physical properties on a dense mesh of Hamiltonian parameters, a requirement for accurate modeling of optical lattice experiments<sup>22,23,37–40</sup> where the confining potential leads to spatially varying chemical potential, interaction strength, and hopping matrix elements.<sup>41</sup> Here we have

shown the potential importance of NLCEs as a tool to analyze pairing in these systems.

## ACKNOWLEDGMENTS

This work was supported by the Department of Energy under DE-NA0001842-0 (EK and RTS), and by the National Science Foundation (NSF) grant number DMR-1306048 (EK and RRPS). This work used the Extreme Science and Engineering Discovery Environment (XSEDE) under project number TG-DMR130143, which is supported by NSF grant number OCI-1053575.

- 
- <sup>1</sup> D. Scalapino, *Does the Hubbard Model Have the Right Stuff? in Proceedings of the International School of Physics*, edited by R. A. Broglia and J. R. Schrieffer (North-Holland, New York, 1994).
  - <sup>2</sup> E. Dagotto, *Rev. Mod. Phys.* **66**, 763 (1994).
  - <sup>3</sup> S. Kivelson, I. Bindloss, E. Fradkin, V. Oganesyan, J. Tranquada, A. Kapitulnik, and C. Howard, *Rev. Mod. Phys.* **75**, 1201 (2003).
  - <sup>4</sup> N. Lee, P.A. amd Nagaosa and X. Wen, *Rev. Mod. Phys.* **78**, 17 (2006).
  - <sup>5</sup> *Handbook of High-Temperature Superconductivity*, edited by J. Robert Schrieffer and James S. Brooks (Springer, New York, 2007).
  - <sup>6</sup> D. Scalapino, *Rev. Mod. Phys.* **84**, 1383 (2012).
  - <sup>7</sup> S. Raghu, S. A. Kivelson, and D. J. Scalapino, *Phys. Rev. B* **81**, 224505 (2010).
  - <sup>8</sup> S. R. White, *Phys. Rev. Lett.* **69**, 2863 (1992).
  - <sup>9</sup> U. Schollwöck, *Rev. Mod. Phys.* **77**, 259 (2005).
  - <sup>10</sup> N. V. Prokof'ev and B. V. Svistunov, *Phys. Rev. Lett.* **81**, 2514 (1998).
  - <sup>11</sup> E. Kozik, K. V. Houcke, E. Gull, L. Pollet, N. Prokof'ev, B. Svistunov, and M. Troyer, *EPL (Europhysics Letters)* **90**, 10004 (2010).
  - <sup>12</sup> S. R. White, D. J. Scalapino, R. L. Sugar, E. Y. Loh, J. E. Gubernatis, and R. T. Scalettar, *Phys. Rev. B* **40**, 506 (1989).
  - <sup>13</sup> C. N. Varney, C.-R. Lee, Z. J. Bai, S. Chiesa, M. Jarrell, and R. T. Scalettar, *Phys. Rev. B* **80**, 075116 (2009).
  - <sup>14</sup> T. Maier, M. Jarrell, T. Pruschke, and M. H. Hettler, *Rev. Mod. Phys.* **77**, 1027 (2005).
  - <sup>15</sup> G. Kotliar, S. Y. Savrasov, G. Pálsson, and G. Biroli, *Phys. Rev. Lett.* **87**, 186401 (2001).
  - <sup>16</sup> E. Y. Loh, J. E. Gubernatis, R. T. Scalettar, S. R. White, D. J. Scalapino, and R. L. Sugar, *Phys. Rev. B* **41**, 9301 (1990).
  - <sup>17</sup> V. I. Iglovikov, E. Khatami, and R. T. Scalettar, *Phys. Rev. B* **92**, 045110 (2015).
  - <sup>18</sup> M. Rigol, T. Bryant, and R. R. P. Singh, *Phys. Rev. Lett.* **97**, 187202 (2006).
  - <sup>19</sup> M. Rigol, T. Bryant, and R. R. P. Singh, *Phys. Rev. E* **75**, 061118 (2007).
  - <sup>20</sup> M. Rigol, T. Bryant, and R. R. P. Singh, *Phys. Rev. E* **75**, 061119 (2007).
  - <sup>21</sup> B. Tang, E. Khatami, and M. Rigol, *Comput. Phys. Commun.* **184**, 557 (2013).
  - <sup>22</sup> R. Hart, P. Duarte, T. Yang, X. Liu, T. Paiva, E. Khatami, R. Scalettar, N. Trivedi, D. Huse, and R. Hulet, *Nature (London)* **519**, 211 (2015).
  - <sup>23</sup> P. Duarte, R. Hart, T. Yang, X. Liu, T. Paiva, E. Khatami, R. Scalettar, N. Trivedi, and R. Hulet, *Phys. Rev. Lett.* **114**, 070403 (2015).
  - <sup>24</sup> R. T. Scalettar, E. Y. Loh, J. E. Gubernatis, A. Moreo, S. R. White, D. J. Scalapino, R. L. Sugar, and E. Dagotto, *Phys. Rev. Lett.* **62**, 1407 (1989).
  - <sup>25</sup> A. Moreo and D. J. Scalapino, *Phys. Rev. Lett.* **66**, 946 (1991).
  - <sup>26</sup> T. Paiva, R. R. dos Santos, R. T. Scalettar, and P. J. H. Denteneer, *Phys. Rev. B* **69**, 184501 (2004).
  - <sup>27</sup> F. Assaad, W. Hanke, and D. Scalapino, *Phys. Rev. B* **49**, 4327 (1994).
  - <sup>28</sup> P. Staar, T. Maier, and T. C. Schulthess, *Phys. Rev. B* **89**, 195133 (2014).
  - <sup>29</sup> H. W. Press, B. P. Flannery, S. A. Teukolsky, and W. T. Vetterling, *Numerical Recipes in Fortran* (Cambridge University Press, Cambridge, England, 1999) Chap. 5.1.
  - <sup>30</sup> A. J. Guttmann, *Phase Transitions and Critical Phenomena*, edited by C. Domb and J. Lebowitz, Vol. 13 (Academic Press, London, 1989).
  - <sup>31</sup> E. Khatami and M. Rigol, *Phys. Rev. A* **84**, 053611 (2011).
  - <sup>32</sup> E. Khatami and M. Rigol, *Phys. Rev. A* **86**, 023633 (2012).
  - <sup>33</sup> B. Tang, T. Paiva, E. Khatami, and M. Rigol, *Phys. Rev. Lett.* **109**, 205301 (2012).
  - <sup>34</sup> In the ninth order alone, we need to distinguish all 1285 clusters that may have the same topology (the same Hamiltonian matrix), but are not related by point group symmetry. The largest matrices to be diagonalized have a linear size of  $N = 15876$ . In the seventh order, there are 108 symmetrically distinct clusters. The largest matrices to be diagonalized here have a linear size of  $N = 3432$ .
  - <sup>35</sup> For example, for the s-wave channel, we have  $P_{\text{corr}}^s(\mathbf{r}_{ij}) = P^s(\mathbf{r}_{ij}) - 2\langle c_{i\sigma}^\dagger c_{j\sigma} \rangle^2 - \delta_{ij} \left[ 1 - 2\langle c_{i\sigma}^\dagger c_{j\sigma} \rangle \right]$ .
  - <sup>36</sup> S. R. White, D. J. Scalapino, R. L. Sugar, N. E. Bickers, and R. T. Scalettar, *Phys. Rev. B* **39**, 839 (1989).

- <sup>37</sup> A. G. Truscott, K. E. Strecker, W. I. McAlexander, G. B. Partridge, and R. G. Hulet, *Science* **291**, 2570 (2001).
- <sup>38</sup> M. Köhl, H. Moritz, T. Stöferle, K. Günter, and T. Esslinger, *Phys. Rev. Lett.* **94**, 080403 (2005).
- <sup>39</sup> U. Schneider, L. Hackermüller, S. Will, T. Best, I. Bloch, T. A. Costi, R. W. Helmes, D. Rasch, and A. Rosch, *Science* **322**, 1520 (2008).
- <sup>40</sup> R. Jördens, N. Strohmaier, K. Günter, H. Moritz, and T. Esslinger, *Nature* **455**, 204 (2008).
- <sup>41</sup> C. J. M. Mathy, D. A. Huse, and R. G. Hulet, *Phys. Rev. A* **86**, 023606 (2012).